Impact of Uncertainty from Load-based Reserves and Renewables on Dispatch Costs and Emissions

Bowen Li
University of Michigan
EECS
libowen@umich.edu

Spencer D. Maroukis
University of Michigan
EECS
smarouki@umich.edu

Yashen Lin
National Renewable Energy Laboratory
yashen.lin@nrel.gov

Johanna L. Mathieu
University of Michigan
EECS
jlmath@umich.edu

***Abstract*—Aggregations of controllable loads are considered to be a fast-responding, cost-efficient, and environmental-friendly candidate for power system ancillary services. Unlike conventional service providers, the potential capacity from the aggregation is highly affected by factors like ambient conditions and load usage patterns. Previous work modeled aggregations of controllable loads (such as air conditioners) as thermal batteries, which are capable of providing reserves but with uncertain capacity. A stochastic optimal power flow problem was formulated to manage this uncertainty, as well as uncertainty in renewable generation. In this paper, we explore how the types and levels of uncertainty, generation reserve costs, and controllable load capacity affect the dispatch solution, operational costs, and CO_2 emissions. We also compare the results of two methods for solving the stochastic optimization problem, namely the probabilistically robust method and analytical reformulation assuming Gaussian distributions. Case studies are conducted on a modified IEEE 9-bus system with renewables, controllable loads, and congestion. We find that different types and levels of uncertainty have significant impacts on dispatch and emissions. More controllable loads and less conservative solution methodologies lead to lower costs and emissions.**

I. Introduction

As more renewable energy is integrated into the power system, more reserves are needed to manage their uncertainty [1]. Aggregations of controllable loads (CLs) are considered to be a promising provider of reserves [2]. Compared with conventional providers, CLs can have shorter response times, lower operational costs, and less environmental impact. However, the potential capacity from the aggregation is uncertain as it can be affected by both ambient conditions and load usage patterns. Previous research has proposed stochastic optimal power flow (OPF) formulations to include uncertain CLs into the dispatch problem [3]–[6]. In those papers, it was assumed that CLs can provide reserves such as regulation (i.e., secondary frequency control) but their available power capacity is uncertain. Despite this uncertainty, it was found that using CLs for reserves can reduce dispatch costs.

The objective of this paper is to determine how load-based reserve uncertainty, in conjunction with renewable uncertainty, affects power system dispatch. With more load-based reserve uncertainty, the system operator will choose to dispatch more expensive but certain reserves from conventional providers, increasing dispatch costs. Through a series of case studies, we investigate how the level and type of uncertainty affect dispatch solutions and operational costs. We also use the dispatch solutions to compute the impact of uncertainty on system CO_2 emissions.

Our case studies use the multi-period chance-constrained DC optimal power flow (CCOPF) formulation developed in [3], [4]. The objective is to co-optimize the day-ahead generation and reserve schedule while satisfying physical constraints. Aggregations of CLs (specifically, electric heat pumps) are modeled as thermal energy storage, and can provide both load shifting and reserves around their baseline power consumption. In this paper, we assume both the baseline and the reserve capacity of the CLs are uncertain and a function of uncertain outdoor air temperature. The problem is stochastic since both renewable (specifically, wind) power forecasts and temperature forecasts are imperfect. The stochastic constraints are formulated as chance constraints, which guarantee the constraints are satisfied with a certain probability. Re-dispatch reserves are scheduled from the conventional generators to correct the energy state of the CLs. To solve the CCOPF, we use two methods – the probabilistically robust method (referred to as "robust") developed by [7] and analytical reformulation assuming Gaussian distributions (referred to as "Gaussian") also implemented in [8], [9] on problems without load-based reserves – and compare the results.

The contributions of this paper are case study results showing how different types and levels of uncertainty, reserve costs, and CL capacity affect power system dispatch, operational costs, and CO_2 emissions. The case studies are conducted on a modified IEEE 9-bus system [10]. We find that different levels of wind and temperature uncertainty significantly change the dispatch, particularly the CLs usage. Reserve costs and congestion also play important roles in determining the dispatch. CO_2 emissions change as the generator dispatch changes. Reserves schedules also affect emissions, but the impact is less significant.

The remainder of the paper is organized as follows. The problem formulation and emissions model are introduced in Section II. Section III introduces the case study setup. Dispatch and emissions results are presented in Section IV. Section V concludes and summarizes future research directions.

II. Problem Formulation

A. Chance-constrained optimal power flow

Due to space limitations, we omit the detailed CCOPF formulation, but provide a brief description here for completeness; the interested reader is referred to [4] for details.

978-1-5090-3270-9/16/$31.00 ©2016 IEEE

The objective is to minimize energy and reserve costs. Supply-demand mismatch stems from uncertainty in wind power production and outdoor air temperature (affecting load). Two types of reserves are scheduled to correct this mismatch: secondary reserves and re-dispatch reserves. The former covers the fast variations in the mismatch, and the latter periodically corrects the slower time-scale mismatch and helps to manage the energy state of CLs providing secondary reserves. Secondary reserves can be provided by both conventional generators and CLs, while the re-dispatch reserves can only be provided by conventional generators. The decision variables in the OPF include the 24-hour generator schedule, CL set point, reserve capacities from both generators and loads, and "distribution vectors" [9], [11] that distribute the real-time supply-demand mismatch to the resources providing reserves. The constraints include generation limits, reserve limits, the DC power flow equations (which must hold for both the forecasted generation/load and with 99% probability for actual generation/load), and load constraints. CLs are assumed to be electric heat pumps, and aggregations of CLs are modeled as thermal energy storage [12]. It is assumed that external control signal are used to switch the heat pumps on/off, ensuring that they stay within narrow range around their temperature set point, and changing their aggregate power consumption $P_{C,t}$. The aggregation's thermal energy state S_t evolves as

$$S_{t+1} = S_t + (P_{C,t} - P_T(T_t))\Delta\tau \tag{1}$$

where t is the time index, $\Delta\tau$ is the time step (e.g., 1 hour), and P_T is the baseline power consumption, which is a function of outdoor air temperature T_t. Both $P_{C,t}$ and S_t are bounded, where the bounds of the former are the thermal battery's "power capacity" and the latter the "energy capacity." The capacities can be computed using the approaches described in [12] and are approximately piecewise linear in P_T (see Fig. 2 of [12]). Here, we model them as exactly piecewise linear. The only difference in the formulation we use in this paper and that of [4] is that here we assume load-based reserves correct both wind error and baseline error (caused by temperature forecast error), whereas in [4] we assumed it only corrected wind error.

We use two methods to solve the CCOPF: the robust method [7] and the Gaussian method [8], [9]. In the robust method, a sample-based robust set is constructed from sufficient scenarios. Then, the problem is solved as a robust optimization problem over the robust set. In the Gaussian method, the uncertainties are assumed to follow Gaussian distributions. The chance constraints are transformed into deterministic constraints, leading to a deterministic optimization problem. In general, the robust method is more conservative than analytical reformulation as it uses sample outliers in the robust set construction.

B. Emissions evaluation

To evaluate the CO_2 emissions we consider i) the emissions from fuel combustion from conventional generators and ii) the emissions from provision of reserves by generators. For i), we assume the hourly fuel consumed is $F(G,t) = f_g(P_{G,t})/k_c$, where $f_g(P_{G,t})$ is the generation cost and k_c is the fuel price. The emissions are then: $E(P_{G,t}) = k_e F(G,t)$, where k_e is the emissions factor. We assume wind generation has no emissions.

When the generator is providing different upward and downward reserves, the actual average output could be different from the dispatch schedule. To evaluate the emissions, we define $P_{e,t} = P_{G,t} + (R_t^{up} - R_t^{dn})/2$, where R_t^{up} and R_t^{dn} are the upward and downward reserves provided by the generator. When the reserves are symmetric (i.e., $R_t^{up} = R_t^{dn}$), then $P_{e,t} = P_{G,t}$.

Generators may produce additional emissions when they change their output quickly to track secondary reserves signals; however, the amount is not well known [13]. In this paper, we let these emissions be: $E_o(R_t^{up}, R_t^{dn}) = \alpha E_m(R_t^{up} + R_t^{dn})$, where E_m is the marginal emissions from the generator at operating at $P_{G,t}$ and α is a scaling factor. In this paper, we take $\alpha = 0.1$; more discussion can be found in [13].

III. Simulation Setup

The testbed is a modified IEEE 9-bus system [10] with a 20 MW capacity wind power plant added to Bus 1. We assume all generators can provide secondary and re-dispatch reserves. Generator costs are taken from the Matpower case file. We choose the "base case" reserve costs as follows: the generator secondary reserve cost is five times the corresponding generator's first-order generation cost, the re-dispatch cost is equal to the generator's first-order cost, and the load reserve cost is 50% of the lowest first-order generator cost (we vary these costs in one of our case studies). To assess CO_2 emissions, we assume the generators at Buses 1 and 3 are gas turbines and at Bus 2 is a coal generator. The fuel price and emission factors can be found in [13]. We use empirical data from [14] for the load profile, which is a bimodal profile with peaks around hours at $t = 10, 20$, which represents a common winter load. We assume that 15% of the load at each bus is controllable but uncertain, and that the uncontrollable load is perfectly forecastable. We set the line flow constraint from Bus 1 to 4 at 50 MW to produce congestion in periods of high demand.

We use the same temperature and wind forecast error uncertainty set as [3], which computed the set from real data. For the robust method, the number of required error samples is determined by the probability of chance constraint violation (here, 1%), a confidence parameter (here, 10^{-4}), and the uncertainty dimension (here, 2) [7]. We draw 2565 uncertainty samples from the set and use them to construct a robust set. For the Gaussian method, we compute the sample mean and covariance of the uncertainty set. Different from [4], we use a conservative approximation for confidence bound (the upper bound, which is labelled "UB" in Fig. 1 of [4]) to simplify the formulation.

We study the impacts of five different factors, listed below, on the system dispatch. We define both a base case and a range for each factor.

1) Wind Forecast Error: As wind forecast error increases, the system needs more reserves. We scale the wind forecast errors by values of $\{0.5, 0.75, 1, 1.25, 1.5\}$, where 1 corresponds to the base case.

2) Temperature Forecast Error: Temperature affects the CL baseline and reserve capacity. As temperature forecast error increases, the system needs more reserves and the CL reserve capacity becomes less certain, requiring more reserves

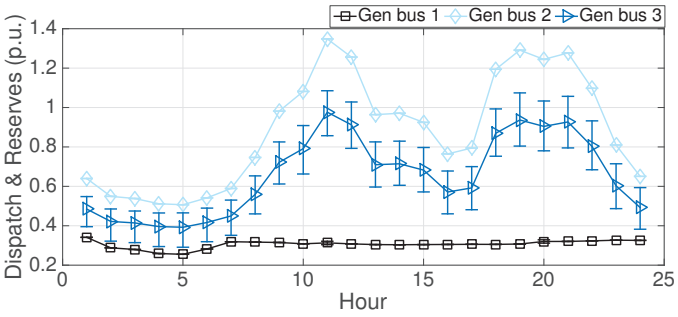

Fig. 1. Generation schedule with re-dispatch reserves for each generator in the base case.

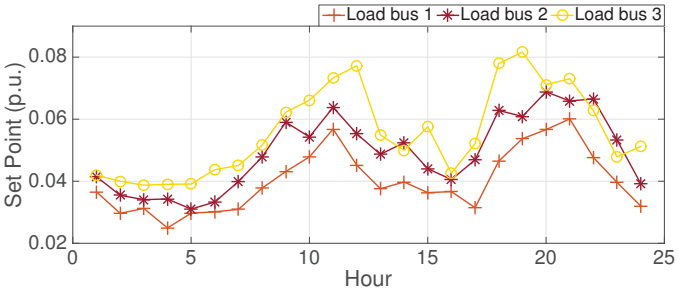

Fig. 2. CL set point for each load in the base case.

from conventional providers. We scale the temperature forecast errors by values of {0.8, 1, 1.2, 1.4, 1.6}.

3) Temperature Forecast: The temperature forecast affects the CL baseline and energy/power capacity. We add an hourly temperature offset of {-10, -5, 0, +5, +10} to the base case forecast.

4) Controllable Load Energy Capacity: To study the impact of the CL's energy capacity, we apply a scaling factor with values of {1, 3.25, 5.5, 7.75, 10}. Increasing the CL's energy capacity (which corresponds to increasing the temperature range within which the heat pumps are allowed to operate) increases the flexibility of the CLs.

5) Reserve Costs: We scale the generator secondary reserve costs by applying a scaling factor with values of {0.02, 0.265, 0.51, 0.755, 1}.

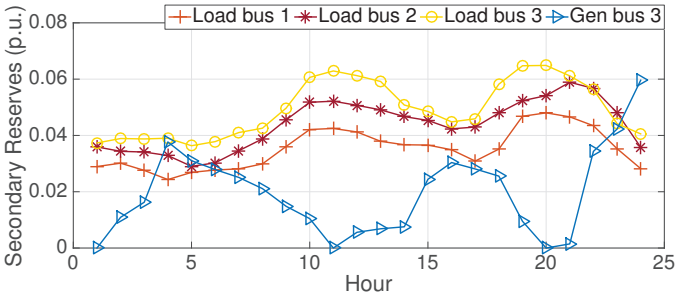

Fig. 3. Secondary reserve capacity provided by generators and loads in the base case.

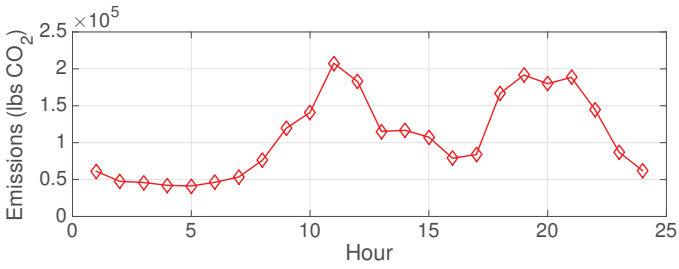

Fig. 4. Hourly CO_2 emissions in the base case.

TABLE I. BASE CASE COSTS & EMISSIONS RESULTS

	Dispatch ($)	Gen. Sec. ($)	Re-dispatch ($)	Load Sec. ($)	Emissions (lbs)
Robust	43371	235.4	528.5	154.1	2.59e+06
Gaussian	43022	0	222.8	72.0	2.54e+06

IV. RESULTS

A. Base Case

The base case results using the robust method are shown in Figs. 1-4. Figure 1 shows the generation dispatch schedule as well as the re-dispatch reserve schedule, where "Gen bus n" refers to generator bus n. We observe that when demand is high, line 1-4 is congested, and the generator on Gen bus 1, which is the lowest cost generator, is limited. Figure 2 shows CL set points for all loads. Figure 3 shows the secondary reserve capacity provided by each generator and load. We observe that load-based reserves are used first due their low cost. When their power or energy capacity is used up, the loads cannot provide more reserves, and so the generators are used to cover the rest of the reserve requirement (we subsequently refer to this as "saturation"). Load-based reserves cover most of the reserve requirement especially during peak hours since the CLs have larger capacities during peak hours. Figure 4 shows the emissions results, which follow a similar trend to the bimodal load profile since most of the emissions are from generator energy production.

Table I summarizes all costs and CO_2 emissions for both the robust method and the Gaussian method. The Gaussian method is less conservative resulting in fewer reserves, which both lowers costs and reduces emissions. The qualitative trends are similar. For example, CLs are used first for secondary reserves. Since fewer reserves are needed, all secondary reserves are provided by the loads.

In the following sections, we present the results associated with varying each factor listed in Section III. In each case, the Gaussian method always produces lower costs and emissions, but similar qualitative results. Therefore, we only present the results for the robust method.

B. Wind Forecast Error

The dispatch costs and emissions difference from the base case (ΔCO_2) and the secondary and re-dispatch reserve costs are shown in Fig. 5. As wind forecast error increases, the reserve requirement increases. We observe that load-based secondary reserves increase until saturation. For low uncertainty, there is no need for generator secondary reserves because the load-based reserves are able to compensate all of the

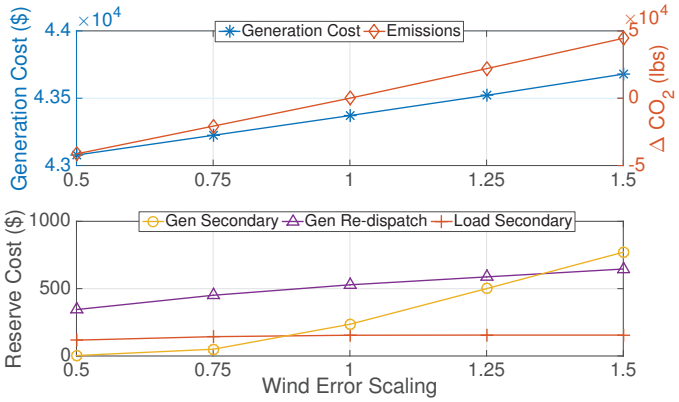

Fig. 5. Dispatch costs and emissions (top) and reserve costs (bottom) for increasing wind forecast error. ΔCO_2 is the emissions difference from the base case.

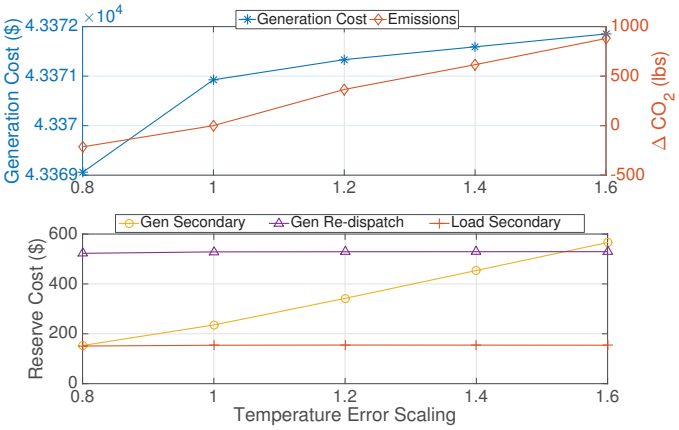

Fig. 6. Dispatch costs and emissions (top) and reserve costs (bottom) for increasing temperature forecast error. ΔCO_2 is the emissions difference from the base case.

error. After load-based reserves saturate, generator secondary reserves are used, and their cost increases linearly with wind error. Generator re-dispatch reserves increase with load-based reserves to recover the CLs' energy states.

Increased wind error also reduces the flow scheduled on line (1-4), ensuring the line constraint will not be violated when the wind forecast uncertainty is high. This results in part of the generation being shifted from Gen bus 1 to the other buses. Since wind generation is also on Gen bus 1, conventional generator dispatch decreases on Gen bus 1 and increases on Gen bus 2 and 3. The CL set points do not change much as wind forecast error increases. This is because, in this case, CLs are mainly used for reserves, not load shifting.

Since generation is shifted from Gen bus 1 to Gen bus 2 and 3, emissions increase significantly as the generator on Gen bus 2 is modeled as a coal generator, which has higher emission factor. There is also an increased asymmetry to the reserves which results in a small increase in emissions.

C. Temperature Forecast Error

The dispatch costs and emissions difference from the base case and the secondary and re-dispatch reserve costs are shown in Fig. 6. As temperature forecast error increases the load-based reserves quickly saturate. Also, more re-dispatch reserves are required to recover the CLs' energy states. The cost increase is smaller compared to that in the wind forecast error case, since temperature forecast error does not induce large power mismatches. As temperature forecast error increases, a greater percentage of load-based reserve capacity is used to compensate temperature forecast error rather than wind forecast error, since the CLs are the only source for temperature foreacast error compensation. This leads to more secondary reserves required from the conventional generators to compensate the wind forecast error. Similar to the wind forecast error case, after load-based reserves saturate, secondary generation reserve costs increase linearly with temperature error.

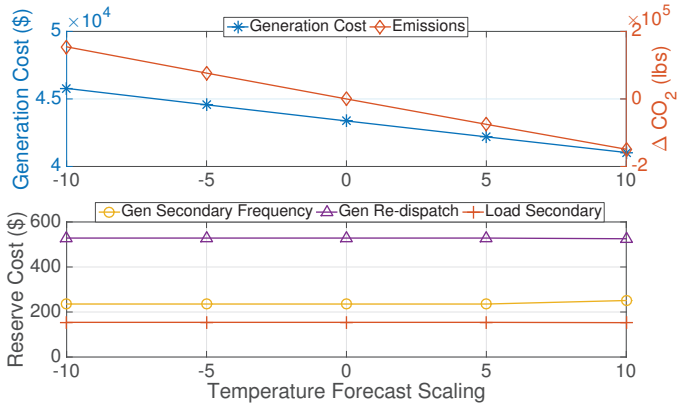

Fig. 7. Dispatch costs and emissions (top) and reserve costs (bottom) for increasing temperature forecast. ΔCO_2 is the emissions difference from the base case.

There is a slight increase in emissions with respect to the base case (total change in emissions for the highest uncertainty case less than 900 lbs CO_2) and mostly due to more reserve usage since the generator dispatch schedule is not significantly affected by temperature error.

D. Temperature Forecast

The dispatch costs and emissions difference from the base case and the secondary and re-dispatch reserve costs are shown in Fig. 7. The CL set points and load-based secondary reserve capacities for Load bus 1 are shown in Fig. 8. As the temperature forecast increases, the generation cost decreases since the CL baseline decreases (i.e., heaters are used less as the temperature increases). The generator on Gen bus 1 is already limited by the line constraint, and so the generators on Gen bus 2 and 3 decrease to match the reduced demand. The load-based reserve costs decrease, the generator secondary reserve costs increase, and the re-dispatch reserves cost decrease for an offset value of 10 since the CLs' power capacities becomes very small; this can be observed in Fig. 8. Emissions reduce with increasing temperature since CL demand reduces, and the change in emissions is dominated by generator dispatch rather than reserves.

E. Controllable Load Energy Capacity

The dispatch costs and emissions difference from the base case and the secondary and re-dispatch reserve costs are

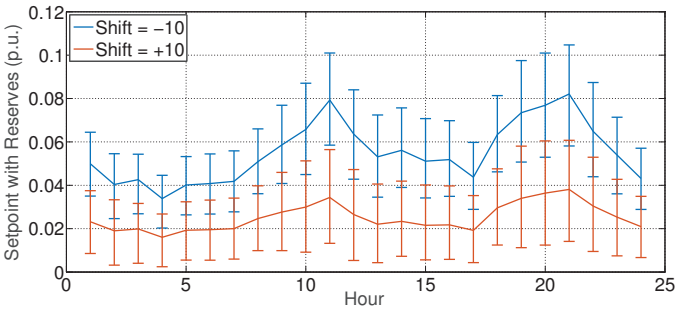

Fig. 8. CL set point and load-based secondary reserves for lowest and highest temperature forecast on Load bus 1.

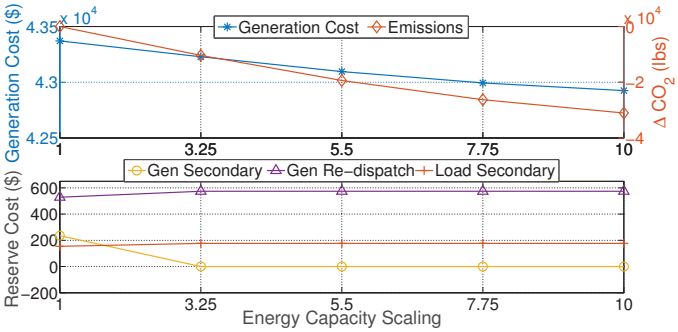

Fig. 9. Dispatch costs and emissions (top) and reserve costs (bottom) for increasing CL energy capacity. ΔCO_2 is the emissions difference from the base case.

shown in Fig. 9. The total load (CL plus uncontrollable load) schedule is shown in Fig. 10. Generation dispatch costs and generation secondary reserve costs decrease as the energy capacities increase since the CLs can provide more reserves and load shifting. While the total CL over the day does not change, an increased energy capacity allows the CL to provide more load shifting, as shown in Fig. 10. The resulting peak shaving reduces operational costs as well as emissions since the marginal cost of generation is higher during peak hours. Load-based reserves increase with increased energy capacity until they provide all reserves. With increased energy capacities, emissions decrease for peak hours and increase for off-peak hours. The total emissions over the 24-hour period show a slight decrease as the CL energy capacity increases.

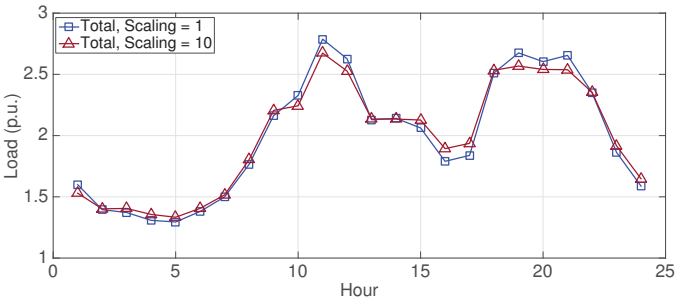

Fig. 10. Total load schedule for lowest and highest energy capacity.

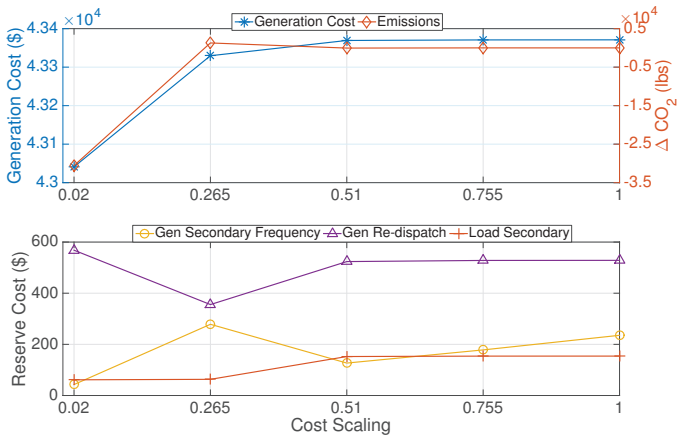

Fig. 11. Dispatch costs and emissions (top) and reserve costs (bottom) for increasing generator secondary reserve cost. ΔCO_2 is the emissions difference from the base case.

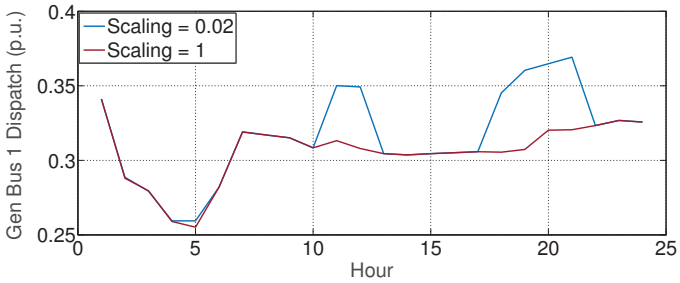

Fig. 12. Generator dispatch for the lowest and highest generator secondary reserve costs on Gen bus 1.

F. *Reserve Costs*

The dispatch costs and emissions difference from the base case and the secondary and re-dispatch reserve costs are shown in Fig. 11. The generation dispatch schedule for Gen bus 1 and secondary reserves provided the generators and loads are shown in Figs. 12 and 13.

In the base case, the generator secondary reserve is more expensive than load-based secondary reserve, and at most times, it is more expensive than the marginal cost of generation. When the scaling is set to 0.02, all generators have cheaper reserve costs than the CLs. Thus generators will be used first to compensate for wind forecast errors. Load-based reserves are still used as they are the only resource used to compensate temperature errors. In this case, during peak hours, the system picks a more expensive reserve provider – the generator on Gen bus 1. This is because the wind generation is also on Gen bus 1 and the line (1-4) is congested. Scheduling reserves on Gen bus 1 allows more power flow be scheduled on the congested line. This shift in generation reduces the generation cost, which is more than the increase in the reserve cost and leads to a lower total cost. CLs are also more effective at load shifting when most of the reserves are provided by generators.

As the scaling factor increases to 0.265, generator secondary reserves still compensate the majority of the wind forecast error due to its low cost. However, during peak hours, Gen bus 1 is no longer used for reserves and Gen bus 3

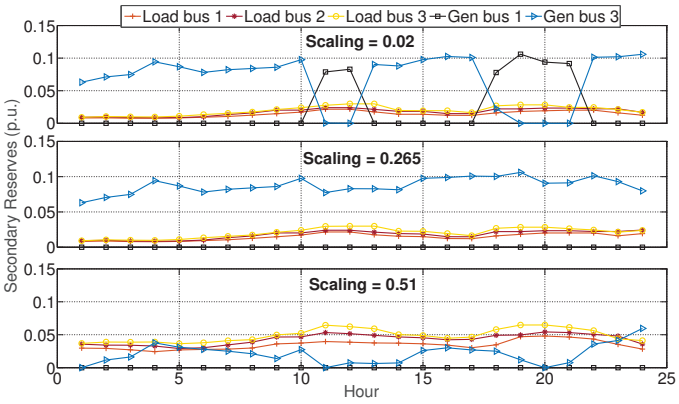

Fig. 13. Secondary reserves for increasing generator secondary reserve costs. The cases with scaling 0.76 and 1 are the same as scaling 0.51 due to CL saturation.

provides secondary and re-dispatch reserves. This is because the reserve cost increase outweighs the congestion relief. With less load-based reserve scheduled, the CLs can help more with load shifting. For scaling factors 0.51 to 1, the CLs will use their full capacity for reserves and become unable to load shift. Hence, we observe an increase in load-based reserve and dispatch costs.

For low generator secondary reserve costs, the generation dispatch is shifted from Gen bus 2 to 1 leading to a reduction in emissions. As generator secondary reserve costs increase, the dispatch is shifted back to Gen bus 2 and more load-based reserves are used. Therefore, we first observe an increase in emissions due to the dispatch shift then a reduction in emissions after load-based reserves saturate.

V. Discussion and Conclusion

In this paper, we performed case studies to investigate the impacts of several factors including load-based reserve uncertainty (i.e., temperature uncertainty), wind uncertainty, reserve costs, and CCOPF solution methodologies on power system dispatch, operational costs, and CO_2 emissions. We find that wind uncertainty has a larger impact on dispatch and emissions than temperature uncertainty. Changes in the temperature forecast highly affect the dispatch schedule and the emissions. Due to their low cost, controllable loads are scheduled to provide reserves before generators are, until they reach their capacity and the generators are needed. We also find that changes in generator dispatch have a more significant impact on the emissions than the changes in the reserve schedule, based on our emissions model. Higher controllable load energy capacities result in more load-based reserves, more load shifting, and reduced emissions. Complicated trade-offs were observed as the generator secondary reserve costs were varied.

The analysis in this paper serves as a first step to quantify the trade-offs between load-based reserve uncertainty and system operational cost, as well as the associated emissions impacts. In future research, we will consider other types of uncertainty that affect controllable load capacity, such as load usage patterns. We will also perform more case studies to find out the impacts of forecast patterns (deviations & peaks) of wind, temperature, and uncontrollable load. The results could provide insights on how to design electricity markets to best utilize controllable loads for reserves.

Acknowledgment

The authors would like to thank M. Vrakopoulou for the wind and temperature uncertainty scenarios. This work was supported by the U.S. National Science Foundation Grant #CCF-1442495.

References

[1] Y. V. Makarov, C. Loutan, J. Ma, and P. de Mello, "Operational impacts of wind generation on california power systems," *Power Systems, IEEE Transactions on*, vol. 24, no. 2, pp. 1039–1050, 2009.

[2] D. S. Callaway and I. A. Hiskens, "Achieving controllability of electric loads," *Proceedings of the IEEE*, vol. 99, no. 1, pp. 184–199, 2011.

[3] M. Vrakopoulou, J. L. Mathieu, and G. Andersson, "Stochastic optimal power flow with uncertain reserves from demand response," in *Proceedings of the Hawaii International Conference on Systems Science (HICSS)*, 2014, pp. 2353–2362.

[4] B. Li and J. L. Mathieu, "Analytical reformulation of chance-constrained optimal power flow with uncertain load control," in *Proceedings of PowerTech, Eindhoven*, 2015, pp. 1–6.

[5] Y. Zhang, S. Shen, and J. Mathieu, "Distributionally robust chance-constrained optimal power flow with uncertain renewables and uncertain reserves provided by loads," *Power Systems, IEEE Transactions on (in press)*, 2016.

[6] G. Martinez, J. Liu, B. Li, J. Mathieu, and C. Anderson, "Enabling renewable resource integration: The balance between robustness and flexibility," in *Proceedings of the Allerton Conference on Communication, Control, and Computing*, Monticello, IL, Oct. 2015.

[7] K. Margellos, P. Goulart, and J. Lygeros, "On the road between robust optimization and the scenario approach for chance constrained optimization problems," *Automatic Control, IEEE Transactions on*, vol. 59, no. 8, pp. 2258–2263, 2014.

[8] L. Roald, F. Oldewurtel, T. Krause, and G. Andersson, "Analytical reformulation of security constrained optimal power flow with probabilistic constraints," in *Proceedings of PowerTech, Grenoble*, 2013.

[9] D. Bienstock, M. Chertkov, and S. Harnett, "Chance-constrained optimal power flow: Risk-aware network control under uncertainty," *SIAM Review*, vol. 56, no. 3, pp. 461–495, 2014.

[10] R. D. Zimmerman, C. E. Murillo-Sánchez, and R. J. Thomas, "Matpower: Steady-state operations, planning, and analysis tools for power systems research and education," *Power Systems, IEEE Transactions on*, vol. 26, no. 1, pp. 12–19, 2011.

[11] M. Vrakopoulou, K. Margellos, J. Lygeros, and G. Andersson, "A probabilistic framework for reserve scheduling and N-1 security assessment of systems with high wind power penetration," *IEEE Transactions on Power Systems*, vol. 28, no. 4, 2013.

[12] J. L. Mathieu, M. Kamgarpour, J. Lygeros, G. Andersson, and D. S. Callaway, "Arbitraging intraday wholesale energy market prices with aggregations of thermostatic loads," *Power Systems, IEEE Transactions on*, vol. 30, no. 2, pp. 763–772, 2015.

[13] Y. Lin, J. X. Johnson, and J. L. Mathieu, "Emissions impacts of using energy storage for power system reserves," *Applied Energy*, vol. 168, pp. 444–456, 2016.

[14] A. Hoke, R. Butler, J. Hambrick, and B. Kroposki, "Steady-state analysis of maximum photovoltaic penetration levels on typical distribution feeders," *Sustainable Energy, IEEE Transactions on*, vol. 4, no. 2, pp. 350–357, 2013.